THE EFFECT OF TERRAIN PROPERTIES ON CRATER MODEL AGE DETERMINATION. M. R. Kirchoff and S. Marchi. Southwest Research Institute, 1050 Walnut St., Suite 300, Boulder, CO 80302. Email: kirchoff@boulder.swri.edu.

Introduction: With the availability of very high resolution and quality imaging from, e.g., Lunar Reconnaissance Orbiter Narrow and Wide Angle Cameras (LROC-NAC/WAC), craters with diameters (D) $\lesssim$ 1 km are now widely used to determine crater model ages of lunar terrains. However, terrain material properties likely alter D $\lesssim$ 5 km crater distributions as indicated by the modern impact scaling law (e.g., Fig. 1, [1-2]). If this is not accounted for, then crater model ages may not be correctly estimated. Note that crater densities at D ~ 1 km traditionally used for determining model ages are within this range. Moreover, crater distributions at smaller diameters obtained from high resolution imaging are even more subject to this effect.

In order to better understand the influence of terrain properties on crater model age assessment, we fit new, expanded crater distributions of Apollo calibration terrains with the Model Production Function (MPF; [2]). The MPF provides the expected number of craters per unit surface per unit time as a function of crater size through converting impactor distributions to crater distributions using modern impact scaling laws, which incorporate terrain properties. Thus, we can use the MPF to find the set of terrain properties that result in a crater model ages that best match the known radiometric ages of examined Apollo terrains. This analysis will provided new constraints on lunar terrain properties, such as material tensile strength, density and porosity, and their affect on estimating crater model ages.

Methods: Because the influence of terrain properties on crater distributions becomes more significant for decreasing crater size (e.g., Fig. 1; [1]), and young terrains' model ages are often extrapolated from D << 1 km craters, it is vital to understand the effect of terrain properties on very small craters. Therefore, we are compiling new, expanded crater distributions for Apollo calibration terrains down to D=10 m (e.g., Fig. 2). To obtain good count statistics for a wide range of diameters, we use a nested technique (e.g., Fig. 3). D $\geq$ 500 m craters are measured within the largest area on the LROC-WAC mosaic (100 m/pixel). The first, second, third, and fourth nested areas use LROC-NAC images to acquire craters for D $\gtrsim$ 250 m, 90 m, 35 m, and 10 m, respectively. Each area is sized to obtain a statistically reasonable number of craters and positioned to include the landing site area and exclude large areas of dense obvious secondaries.

Once the cumulative crater size-frequency distributions (SFDs) are compiled using standard techniques [3], we quantitatively fit them with distinct MPFs that

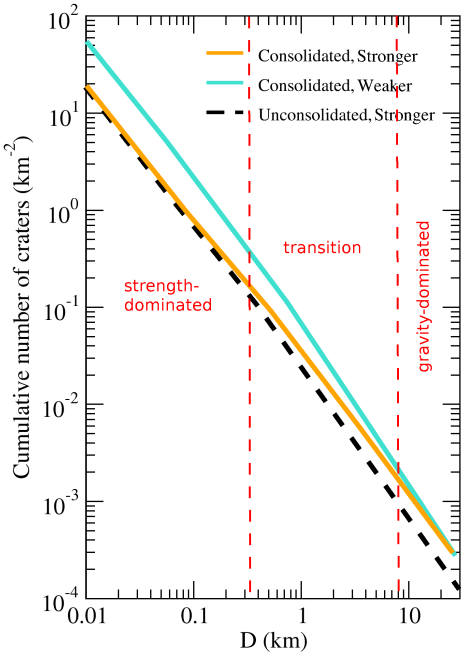

Figure 1. *Crater distributions resulting from different terrain properties in the crater scaling law [1-2]. The transition from the strength- to gravity-dominated regime is gradual and occurs over D~0.3-10 km.*

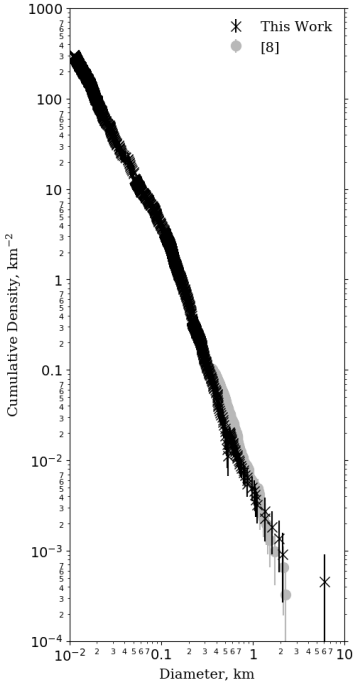

Figure 2. *Comparison of an extended crater distribution from this work to a recent compilation by [8] for Mare Imbrium (Apollo 15).*

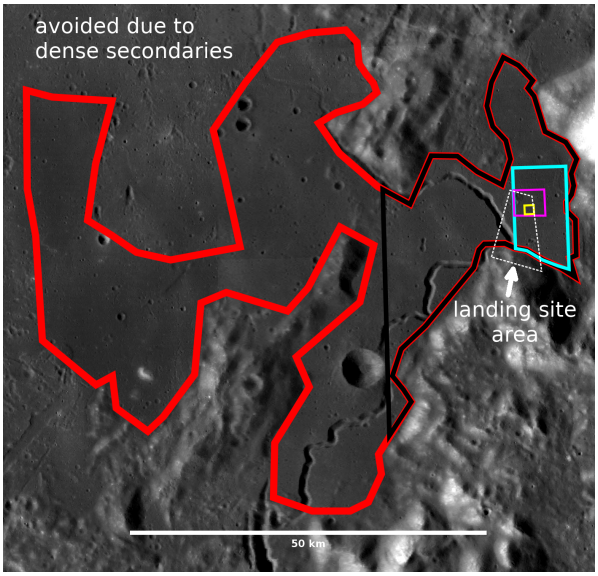

Figure 3. *Example of nested technique for Mare Imbrium. Red outline indicates largest area measured on WAC mosaic. Black outline indicates first nest, cyan for second, magenta for third, and yellow for fourth. Used NAC images are shown. Landing site area is indicated by white dashed outline. North is up.*

use broadly different terrain properties. Terrain properties are varied through coarsely altering the parameters in the crater scaling law [1] that represent material type (consolidated, unconsolidated, porous), material tensile strength, and material density (for further details see [2]). The fits output crater retention ages for the terrain, which are then compared to the known radiometric age [4]. We find which terrain properties produce the best match in ages, and assess what the implications are for the mapped terrains.

Preliminary Results and Future Work: Fig. 4 shows preliminary results for Mare Imbrium (Apollo 15 sample age: 3.3 Ga; [4]). The green line represents the current best MPF fit to the compiled cumulative crater SFD (black x's) that reproduces the radiometric age. This fit is weighted to favor the data for D ≥ 100 m, since craters smaller than this are likely in saturation equilibrium (as represented by the gray line; [5]). We recognize that the smallest craters will likely be saturated for most terrains. Nevertheless, since the diameter at which saturation occurs varies with age, we compile all distributions down to D = 10 m to determine that limit, and we use as much data as possible.

The current best MPF fit uses crater scaling law parameters [1] for consolidated rock (μ=0.55 and ρ=3.5 g/cm^3) with a tensile strength of 2x10^7 dyne/cm^2. Since intact rock has a strength of 2x10^8 dyne/cm^2 [6], our fit would indicate the material is somewhat fractured rock (at the scale of craters considered here, ~100 m laterally and ~20 m depth), as expected for a basalt flow of this age. If other tensile strengths are used (with the same consolidated parameters) implying more or less fractured rock, the model age does not match the radiometric age and is off by ≥200 Myrs [7].

This result demonstrates we can use the MPF with Apollo calibration terrains to better understand how terrain properties affect estimating crater model ages. We will continue to use this approach to further constrain the terrain properties of Mare Imbrium and other Apollo terrains including Mare Tranquillitatis from Apollo 11, Oceanus Procellarum and Copernicus crater from Apollo 12, Fra Mauro Formation of Apollo 14, Cayley Formation of Apollo 16, and Mare Serenitatis/ Taurus Littrow of Apollo 17.

References: [1] Holsapple K.A. and Housen K.R. (2007) *Icarus*, *187*, 345–356. [2] Marchi S. et al. (2009) *AJ*, *137*, 4936–4948. [3] CATWG (1979) *Icarus*, *37*, 467–474. [4] Stöffler D. et al. (2006) *Rev. Min. Geo.*, *60*, 519–596. [5] Hartmann W.K. (1984) *Icarus*, *60*, 56–74. [6] Asphaug, E. et al. (1996) *Icarus*, *120*, 158–184. [7] Kirchoff M.R. et al. (2015) *46th LPSC*, Abst. #2121. [8] Robbins S.J. (2014) *EPSL*, *403*, 188–198.

Acknowledgements: This work is supported by LDAP grant #NNX16AN52G.

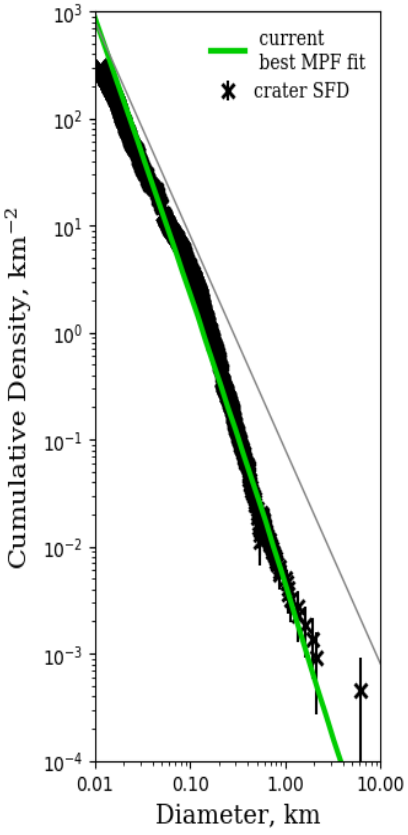

Figure 4. *Current best MPF fit to cumulative crater SFD for Mare Imbrium. Gray line indicates 2% geometric saturation.*